

# Definition by Functional and Structural Analysis of Two Malonyl-CoA Sites in Carnitine Palmitoyltransferase 1A<sup>\*[S]</sup>

Received for publication, January 30, 2007, and in revised form, April 17, 2007. Published, JBC Papers in Press, April 23, 2007, DOI 10.1074/jbc.M700885200

Eduardo López-Viñas<sup>†||1</sup>, Assia Bentebibel<sup>§||1</sup>, Chandrashekar Gurunathan<sup>§||1</sup>, Montserrat Morillas<sup>§||2</sup>, Dolores de Arriaga<sup>¶</sup>, Dolors Serra<sup>§||</sup>, Guillermina Asins<sup>§||</sup>, Fausto G. Hegardt<sup>‡||3</sup>, and Paulino Gómez-Puertas<sup>‡||</sup>

From the <sup>†</sup>Centro de Biología Molecular “Severo Ochoa” (Consejo Superior de Investigaciones Científicas-Universidad Autónoma de Madrid), Cantoblanco, E-28049 Madrid, Spain, <sup>§</sup>Departamento de Bioquímica y Biología Molecular, Facultad de Farmacia, Universidad de Barcelona, E-08028 Barcelona, Spain, <sup>¶</sup>Departamento de Biología Molecular, Universidad de León, E-24071 León, Spain, and <sup>||</sup>CIBER Institute of Fisiopatología de la Obesidad y Nutrición (CB06/03), Instituto de Salud Carlos III, 28049 Madrid, Spain

Carnitine palmitoyltransferase 1 (CPT1) catalyzes the conversion of palmitoyl-CoA to palmitoylcarnitine in the presence of L-carnitine, thus facilitating the entry of fatty acids to mitochondria, in a process that is physiologically inhibited by malonyl-CoA. To examine the mechanism of CPT1 liver isoform (CPT1A) inhibition by malonyl-CoA, we constructed an *in silico* model of both its NH<sub>2</sub>- and COOH-terminal domains. Two malonyl-CoA binding sites were found. One of these, the “CoA site” or “A site,” is involved in the interactions between NH<sub>2</sub>- and COOH-terminal domains and shares the acyl-CoA hemitunnel. The other, the “opposite-to-CoA site” or “O site,” is on the opposite side of the enzyme, in the catalytic channel. The two sites share the carnitine-binding locus. To prevent the interaction between NH<sub>2</sub>- and COOH-terminal regions, we produced CPT1A E26K and K561E mutants. A double mutant E26K/K561E (swap), which was expected to conserve the interaction, was also produced. Inhibition assays showed a 12-fold decrease in the sensitivity (IC<sub>50</sub>) toward malonyl-CoA for CPT1A E26K and K561E single mutants, whereas swap mutant reverts to wild-type IC<sub>50</sub> value. We conclude that structural interaction between both domains is critical for enzyme sensitivity to malonyl-CoA inhibition at the “A site.” The location of the “O site” for malonyl-CoA binding was supported by inhibition assays of expressed R243T mutant. The model is also sustained by kinetic experiments that indicated linear mixed type malonyl-CoA inhibition for carnitine. Malonyl-CoA alters the affinity of carnitine, and there appears to be an exponential inverse relation between carnitine *K<sub>m</sub>* and malonyl-CoA IC<sub>50</sub>.

Carnitine palmitoyltransferase 1 (CPT1)<sup>4</sup> catalyzes the conversion of long-chain fatty acyl-CoAs to acylcarnitines in the presence of L-carnitine. This is the first step in the transport of long-chain fatty acids from the cytoplasm to the mitochondrial matrix, where they undergo  $\beta$ -oxidation. CPT1 is tightly regulated by its physiological inhibitor malonyl-CoA. This regulation allows CPT1 to signal the availability of lipid and carbohydrate fuels to the cell (1). Mammalian tissues express three isoforms: CPT1A (liver), CPT1B (muscle and heart), and CPT1C (brain), which are the products of different genes (2–4). CPT1A and -B have 62% amino acid identity, but they are differentially regulated by malonyl-CoA. CPT1A is inhibited to a much lesser extent than CPT1B, which may explain why fatty acid oxidation is more finely regulated in the heart than in the liver. CPT1 is a potential target for the treatment of metabolic disorders involving diabetes and coronary heart disease (5). The interaction between malonyl-CoA and CPT1C may be involved in the “malonyl-CoA signal” in hypothalamic neurons regulating food intake and peripheral energy expenditure (6).

It has been postulated that there are two malonyl-CoA binding sites in the molecule of CPT1A (7, 8). Kinetic studies indicate that there is a high affinity binding site and a low affinity binding site (9–13). The probable binding sites of malonyl-CoA in CPT1A were deduced to be at the COOH terminus, after the preparation of several CPT1A and CPT1B chimeras (14). Our group has reported that the conserved Met<sup>593</sup>, which is located in the COOH-terminal domain, plays a critical permissive role in the interaction between the enzyme and malonyl-CoA. The mutation of this amino acid to serine abolished the malonyl-CoA sensitivity of CPT1A (15). However, the NH<sub>2</sub> terminus of CPT1A (residues 1–47) was also shown to influence the enzyme/inhibitor interaction. Mutation of either Glu<sup>3</sup> or His<sup>5</sup> reduced malonyl-CoA sensitivity (12, 16). In addition, the removal of the segment comprised between amino acids 3 and 18 in both CPT1A and CPT1B decreased sensitivity to malonyl-CoA, which emphasizes the importance of the NH<sub>2</sub> terminus before the first transmembrane region as a modulator of malonyl-CoA inhibition (17). Further, it has been demon-

\* This study was supported by Dirección General de Investigación Científica y Técnica, Spain, Grants BMC2001-3048 and SAF2004-06843; Ajut de Suport als Grups de Recerca de Catalunya Grant 2005SGR-00733 (to F. G. H.); and a grant from Fundació Ramón Areces (to the Centro de Biología Molecular “Severo Ochoa”). The costs of publication of this article were defrayed in part by the payment of page charges. This article must therefore be hereby marked “advertisement” in accordance with 18 U.S.C. Section 1734 solely to indicate this fact.

[S] The on-line version of this article (available at <http://www.jbc.org>) contains supplemental Table S1.

<sup>1</sup> Both authors contributed equally to this work.

<sup>2</sup> Present address: Dept. de Ciències Experimentals y de la Salut, Universitat Pompeu Fabra, Parc de Recerca Biomèdica de Barcelona, E-08003 Barcelona, Spain.

<sup>3</sup> To whom correspondence should be addressed: Dept. of Biochemistry and Molecular Biology, University of Barcelona, School of Pharmacy, Diagonal 643, E-08028 Barcelona, Spain. E-mail: fgarciaheg@ub.edu.

<sup>4</sup> The abbreviations used are: CPT1, carnitine palmitoyltransferase 1; CPT1A, carnitine palmitoyltransferase 1 liver isoform; CPT1B, carnitine palmitoyltransferase 1 muscle isoform; CPT2, carnitine palmitoyltransferase 2.

strated by a physico-chemical method that CPT1A adopts different conformational states that are more or less sensitive to malonyl-CoA inhibition. These conformational states also involve different degrees of proximity between specific residues within the NH<sub>2</sub>- and COOH-terminal domains in conditions characterized by changes in malonyl-CoA sensitivity (18). Moreover, it has recently been observed that changes (whether insertions or deletions) in the length of the loop proximal to the transmembrane 2 region of CPT1A can increase its sensitivity to malonyl-CoA (19).

Several authors report data relating the inverse association between the effects of malonyl-CoA and carnitine on CPT1 activity. These can be summarized as follows: 1) in liver, the inhibitory effect of malonyl-CoA on CPT1 activity is weaker after starvation and ketosis, when the carnitine content of the cell increases (20, 21); 2) tissues in which CPT1 is most sensitive to malonyl-CoA (muscle and heart) require the highest concentration of carnitine to drive the reaction (22); 3) there is a reciprocal relationship between the affinity of carnitine and malonyl-CoA concentration, since malonyl-CoA increases the  $K_m$  of the enzyme for carnitine, and hence the inhibitory effect of malonyl-CoA varies with carnitine concentration (11, 23); 4) mutations designed to decrease malonyl-CoA sensitivity increase catalytic efficiency of CPT1 for carnitine, which appears to be roughly proportional to the extent of the alteration in malonyl-CoA sensitivity (15). This indicates that such mutants can position carnitine better at the catalytic site, thus displacing malonyl-CoA and reducing the inhibition of CPT1.

Since CPT1 has not been crystallized, many attempts have been made to identify the domains in CPT1 that may bind malonyl-CoA. However, the location of such binding sites has not yet been reported. In the present paper, we describe two putative binding sites for malonyl-CoA in rat CPT1A. They were inferred from the analysis of computational docking models developed for this interaction. The presence of malonyl-CoA on the protein-ligand interaction sites interferes with the positioning of carnitine. One of the sites, the "CoA site" or "A site," is involved in the interactions between its NH<sub>2</sub>- and COOH-terminal domains, and the other, "opposite-to-CoA site" or "O site," only intervenes in the COOH-terminal domain. Mutations of specific amino acids from both NH<sub>2</sub> and COOH termini support their involvement in CPT1 malonyl-CoA sensitivity.

This model is also supported by kinetic experiments that indicated linear mixed type malonyl-CoA inhibition for carnitine, suggesting that the positioning of malonyl-CoA near to the carnitine binding locus produces competitive-non-competitive inhibition. Furthermore, a linear inverse correlation between the logarithm of the IC<sub>50</sub> for malonyl-CoA and the logarithm of  $K_m$  for carnitine was observed. Overall, these data indicate a close relationship between the effects of malonyl-CoA on CPT1 and its affinity for carnitine. This conclusion is supported not only by experimental data but also by the two putative binding sites for malonyl-CoA in the three-dimensional structural model of CPT1A deduced from docking calculations.

## EXPERIMENTAL PROCEDURES

**Construction of Site-directed Mutants**—Plasmids, pYESLCPTI<sup>E26K</sup>, pYESLCPTI<sup>K561E</sup>, pYESLCPTI<sup>R45D</sup>, pYESLCPTI<sup>D698R</sup>, and pYESLCPTI<sup>R243T</sup> were constructed using the QuikChange PCR-based mutagenesis procedure (Stratagene) with the plasmid pYESLCPTI<sup>wt</sup>, obtained as previously described (15), as template. Plasmids containing double mutations pYESLCPTI<sup>E26K/K561E</sup>, pYESLCPTI<sup>R45D/D698R</sup>, and pYESLCPTI<sup>R243T/A478G</sup> were constructed using the same procedure with the plasmids pYESLCPTI<sup>E26K</sup>, pYESLCPTI<sup>R45D</sup>, and pYESLCPTI<sup>R243T</sup> as templates, respectively. The primers used for PCR are described in supplemental Table 1. The appropriate substitutions and the absence of unwanted mutations were confirmed by sequencing the inserts in both directions with an Applied Biosystems 373 automated DNA sequencer.

**Expression of CPT1A in *Saccharomyces cerevisiae***—The expression of the constructs containing wild type and mutants CPT1A in yeast cells and the preparation of the cell extracts were performed as described elsewhere (15). *S. cerevisiae* was chosen as an expression system for wild type and mutant CPT1A, because it does not have endogenous CPT1A activity.

**Determination of Carnitine Acyltransferase Activity**—Carnitine palmitoyltransferase activity was determined by the radiometric method as described elsewhere (15) with minor modifications. The substrates were L-[methyl-<sup>3</sup>H]carnitine and palmitoyl-CoA. Enzyme activity was assayed for 4 min at 30 °C in a total volume of 200 μl.

Substrate saturation data were fitted to rectangular hyperbolic by nonlinear regression using the program EnzFitter (BioSoft).  $K_m$  was estimated by analyzing the data from three experiments. For determination of the apparent  $K_m$  for carnitine, palmitoyl-CoA concentration was fixed at 135 μM, and for determination of the  $K_m$  for palmitoyl-CoA, carnitine concentration was fixed at 400 μM.

When malonyl-CoA inhibition was assayed, increasing concentrations of malonyl-CoA comprised between 0.05 and 100 μM were included. The IC<sub>50</sub>, defined as the malonyl-CoA concentration that produces 50% inhibition of enzyme activity, was determined at 50 μM palmitoyl-CoA and 400 μM carnitine. IC<sub>50</sub> was calculated by Excel software using linear regression analysis.

Values reported here are the means and S.D. of 3–5 determinations. Curve fitting was carried out using Sigma plot software version 8.0. All protein concentrations were determined using the Bio-Rad protein assay with bovine albumin as a standard.

**Immunological Techniques**—Western blot analysis of wild type CPT1A and the assayed mutants using polyclonal antibodies was performed as described (24). The antibody for rat CPT1A was kindly given by Dr. C. Prip-Buus (Institut Cochin, Université René Descartes, Paris, France) and was directed against peptide 317–430, in the cytosolic catalytic C-terminal domain. For the CPT1A wild type and mutants, proteins of predicted sizes were synthesized with similar levels of expression.

## Two Separate Sites for Malonyl-CoA Inhibition of CPT1A

**Search of Homologous Proteins of Rat CPT1A Amino-terminal Domain**—In order to find structural homologues for the amino-terminal domain sequence of rat CPT1A, the FFAS03 server (25, 26) facilities were used on the World Wide Web at [ffas.ljcrf.edu/ffas-cgi/cgi/ffas.pl](http://ffas.ljcrf.edu/ffas-cgi/cgi/ffas.pl). The PSI-BLAST (27)-based profile-profile comparisons were performed against the SCOP data base (28, 29) as a source of protein classification. From the output set of possible structural homologues among the SCOP data base representatives, the best candidate structure in terms of the FFAS03 server's empirical evaluation of matching significance was selected for further three-dimensional model building.

**Three-dimensional Protein Modeling of the CPT1A Amino- and Carboxyl-terminal Domains**—The structural model for the rat CPT1A amino-terminal domain was assembled using homology modeling procedures, supported on the profile-based sequence alignment from the FFAS03 server output, and using the Protein Data Bank (30) coordinates of the selected structural homologue (1TF3; *Xenopus laevis* transcription factor IIIa (31)) as three-dimensional template. The structural model for rat CPT1A carboxyl-terminal domain was constructed using homology modeling procedures based on multiple structure-based amino acid sequence alignments of the carnitine acyltransferase family and the crystallographic coordinates of carnitine octanoyltransferase bound to acylcarnitine (Protein Data Bank entry 1XL8, chain A) (32) and carnitine palmitoyltransferase 2 (Protein Data Bank entry 2H4T) (33). Structural three-dimensional models were built using the SWISS-MODEL server (34–36) facilities on the World Wide Web at [www.expasy.ch/swissmod/SWISS-MODEL.html](http://www.expasy.ch/swissmod/SWISS-MODEL.html), and their structural quality was checked using the WHAT-CHECK routines (37) from the WHAT IF program (38) from the same server. Finally, in order to optimize geometries, release local constraints, and correct possible inappropriate contacts, the modeled structures were energy-minimized with the implementation of the GROMOS 43B1 force field in the program DeepView (39), using 500 steps of steepest descent minimization followed by 500 steps of conjugate-gradient minimization.

**CPT1A Amino- and Carboxyl-terminal Domain Structural Interaction**—The structural model for the molecular interaction between rat CPT1A amino- and carboxyl-terminal domains was built using the computational methods for protein-protein rigid docking implemented in the program Hex (40). In order to reduce the complexity of the 6D positional search between both protein structures, the initial relative positioning of the amino-terminal domain was restrained to the CoA binding pocket side of the carboxyl terminal as proposed by Faye *et al.* (18). For all of the docking models generated, molecular mechanics energy minimization over the force field implemented in Hex was finally performed. From the overall models, the best complex in terms of highest steric and electrostatic correlation between the pair of protein structures was selected.

**Malonyl-CoA Molecular Docking**—In order to obtain a structural model of the interaction between CPT1A and its principal physiological inhibitor malonyl-CoA, molecular docking procedures between both structures were performed using the

methods implemented in the program suite Autodock 3.0 (41–43) as described previously (44).

## RESULTS

**Structural Model for the CPT1A NH<sub>2</sub>-terminal Domain and Its Interaction with the COOH-terminal Domain**—Both NH<sub>2</sub>- and COOH-terminal domains of CPT1A are implicated in modulating the enzyme sensitivity to malonyl-CoA. To study the nature of the suggested interactions between the two regions and to determine how such interactions can influence the role of malonyl-CoA, we constructed *in silico* structural models of both domains and their structural contacts. We constructed a three-dimensional model of the residues in the NH<sub>2</sub>-terminal domain, comprising amino acids 1–61 of human CPT1A. Classic homology-based modeling techniques failed to provide a feasible template for the NH<sub>2</sub>-terminal domain, due to the lack of a close relative of known structure that could be detected using a simple BLAST search in the Protein Data Bank. To overcome this difficulty, an iterative procedure was implemented through the use of the FFAS03 server based on PSI-BLAST profile-profile searching against the classified protein structure data base SCOP as described under “Experimental Procedures.” Iterative techniques like PSI-BLAST allow a more extensive search through sequence databases for remote homologues, usually maintaining structural constraints in terms of secondary and three-dimensional organization in the absence of high sequence identity. The first hit obtained on the FFAS03 server was the SCOP region *d1tf3a3*, corresponding to the three-dimensional structure of the  $\alpha 3$  domain of the three-dimensional structure of *X. laevis* transcription factor IIIA (Protein Data Bank code 1TF3 (31)), with a score of  $-6.860$  and a sequence identity of 50% over an alignment length of 44 residues; this result was within the limits of the technique. A structure-based multiple sequence alignment of several CPT1A and CPT1B NH<sub>2</sub>-terminal sequences and the sequence of the Protein Data Bank structure 1TF3 is shown in Fig. 1A.

Using the crystallographic coordinates of 1TF3 as template and the information obtained from the structural alignment between 1TF3 and the NH<sub>2</sub>-terminal sequences of CPT1, a three-dimensional model was constructed for human CPT1A residues 10–50 (Fig. 1B). The model shows four  $\beta$  strands (E1, residues 12–14; E2, residues 20–22; E3, residues 27–30; E4, residues 34–37) and an  $\alpha$  helix (H1, residues 38–47). The first two strands and the helix were completely aligned with the template, but beta strands E3 and E4 were modeled with less structural confidence. A model for the COOH-terminal domain of human CPT1A was constructed over the crystallographic structure of mouse carnitine octanoyltransferase (32) and CPT2 (33) using standard homology modeling-based techniques, as described elsewhere (45).

Having obtained three-dimensional models both for NH<sub>2</sub>- and COOH-terminal domains of CPT1A, we then used the resulting structures to build a model for the putative interaction between them, using the *in silico* method Hex for protein-protein rigid docking, as described under “Experimental Procedures.” Initial positioning of both protein domains was selected on the basis of the relative location on the NH<sub>2</sub>-terminal domain in the nucleotide fragment of the

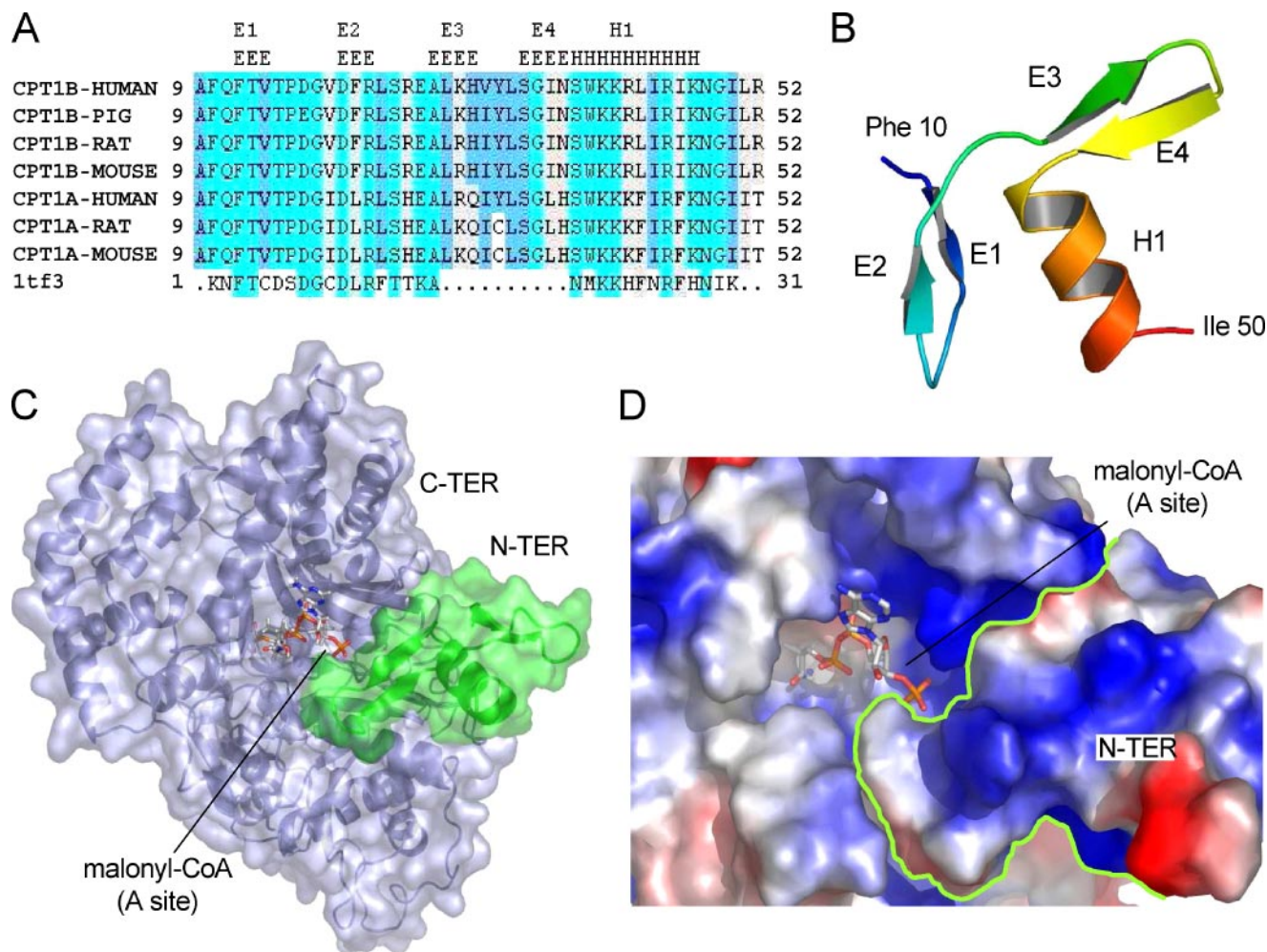


**FIGURE 1. Structural model for NH<sub>2</sub>- and COOH-terminal domains of CPT1A.** *A*, structural alignment colored according to conservation of NH<sub>2</sub>-terminal domains of CPT1A and CPT1B sequences obtained from several organisms. The sequence of Protein Data Bank structure 1TF3 (*X. laevis* transcription factor IIIA) is included for comparison. Secondary structure elements of the NH<sub>2</sub>-terminal domain model are also indicated. *B*, structural model of human CPT1A residues 10–50. The position of predicted structural elements is indicated. *C*, using *in silico* docking procedures for prediction of protein-protein and protein-ligand interaction, a putative complex between NH<sub>2</sub>- (green) and COOH-terminal (blue) domains of human CPT1A was used to predict a site for malonyl-CoA binding at the substrate cavity of the molecule. *D*, detail of the interaction site showing the electrostatic characteristics of the surrounding area. The boundary between NH<sub>2</sub>- and COOH-terminal domains has been highlighted. Protein representations were performed using PyMOL (DeLano Scientific, San Carlos CA).

**TABLE 1**

**Residues involved in the interactions between NH<sub>2</sub>- and COOH-terminal domains of human CPT1A**

Listed are residues in the modeled NH<sub>2</sub>-terminal domain of human CPT1A located at less than 4 Å from the surface of the COOH-terminal domain and their interacting counterparts.

NH <sub>2</sub> -terminal	COOH-terminal	Interactions
Phe <sup>10</sup>	Glu <sup>729</sup> , Asn <sup>730</sup>	Amide of Phe <sup>10</sup> interacts with the partially charged carboxylic oxygen in Glu <sup>729</sup> and with the Asn <sup>730</sup> carboxamide side chain.
Gln <sup>11</sup>	Glu <sup>729</sup> , Asn <sup>730</sup>	The triad of residues Phe <sup>10</sup> -Gln <sup>11</sup> -Phe <sup>12</sup> is conserved in CPT1A and CPT1AB NH <sub>2</sub> -terminal domain multiple sequence alignment.
Phe <sup>12</sup>	Gly <sup>728</sup> , Glu <sup>729</sup>	The triad of residues Gly <sup>728</sup> -Glu <sup>729</sup> -Asn <sup>730</sup> is conserved in CPT1A, CPT1B, and CPT1C sequences.
Ser <sup>24</sup>	Gly <sup>728</sup> , Glu <sup>729</sup>	Pair Gly <sup>728</sup> -Glu <sup>729</sup> , as well as Ser <sup>24</sup> , is conserved in all CPT1 sequences.
His <sup>25</sup>	Lys <sup>556</sup> , Gly <sup>557</sup> , Gly <sup>728</sup>	Lys <sup>556</sup> is in contact with the modeled position of malonyl-CoA.
Glu <sup>26</sup>	Lys <sup>561</sup>	The side-chain carboxyl group of Glu <sup>26</sup> is in contact with the amino group of Lys <sup>561</sup> .
Leu <sup>28</sup>	Lys <sup>556</sup> , Lys <sup>560</sup>	Lys <sup>556</sup> and Lys <sup>560</sup> show a contact between their respective hexanoyl side-chain groups and the N-terminal hydrophobic residue Leu <sup>28</sup> .
Ile <sup>31</sup>	Ser <sup>299</sup> , Gly <sup>298</sup>	Ile <sup>31</sup> is in contact with the proposed site for malonyl-CoA.
Gln <sup>30</sup>	Gln <sup>693</sup>	Gln <sup>693</sup> is located on the external side of the elongated loop, positioned between β strands E13 and E14 and present only in CPT1, which wraps the internal palmitoyl cavity (45).
Tyr <sup>32</sup>	Pro <sup>293</sup> , Arg <sup>295</sup> , Leu <sup>296</sup>	Tyr <sup>32</sup> is in contact with Ile <sup>31</sup> , which is proposed to interact with malonyl-CoA.

acyl-CoA binding face (18). We selected the model with the highest score in terms of steric and electrostatic correlation, and we applied energy minimization steps to correct unrealistic contacts. The final model for the NH<sub>2</sub>-terminal domain

on the surface of COOH-terminal CPT1A structure is shown in Fig. 1, *C* and *D*. Table 1 summarizes the residues involved in the interactions between NH<sub>2</sub>- and COOH-terminal domains.

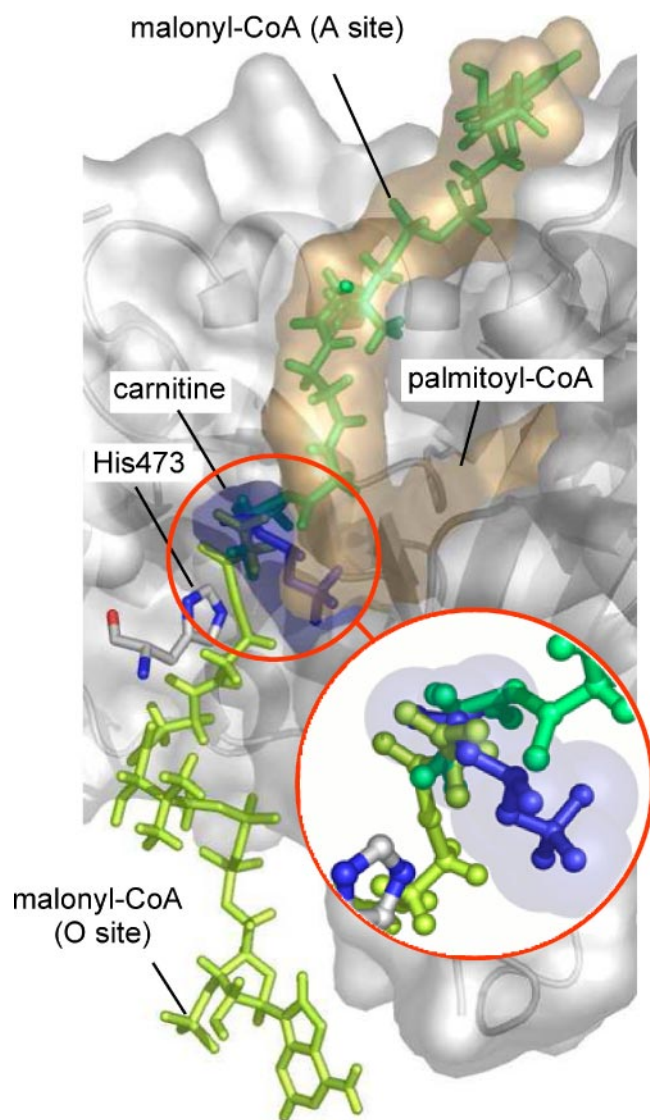


FIGURE 2. **Two sites for malonyl-CoA binding to CPT1A.** Longitudinal section of CPT1A structure illustrating the two putative binding loci for malonyl-CoA: A site (dark green) and O site (light green). The loci of substrates palmitoyl-CoA (shaded yellow) and carnitine (shaded blue) are shown. A molecule of carnitine (blue) in the active site of the enzyme is shown to illustrate the interference of the malonyl-CoA molecule (in both orientations). The position of catalytic residue His<sup>473</sup> is also indicated. The inset shows in detail the predicted clashes between carnitine and malonyl moieties of malonyl-CoA molecules.

*In Silico Docking of the Malonyl-CoA Molecule in CPT1A Structure*—The final docking model for interacting NH<sub>2</sub>- and COOH-terminal domains in human CPT1A was used as a structural frame to perform a search for a putative location of both substrates carnitine and palmitoyl-CoA and the physiological inhibitor malonyl-CoA in the active center of the enzyme. A three-dimensional model of the free malonyl-CoA molecule was prepared using molecular-orbital calculation methods implemented in Mopac (46), and then low energy conformational *in silico* models for putative inhibitor positions were generated and evaluated applying the algorithms AutoGrid and Autodock (see “Experimental Procedures”). Two runs of Autodock3 using the LGA algorithm rendered 200 conformations that were clustered with a root mean square deviation cut-off of 1 Å for all atoms of each docked solution, discarding unrealistic solutions. Docking methodology rendered a binding site for malonyl-CoA close to the interaction of NH<sub>2</sub>- and COOH-terminal domains, and residues from both domains were implicated (Figs. 1 and 2). A putative second site for the inhibitor molecule, located on the opposite side of the molecule, was also predicted (Fig. 2). In both models, the best docked conformation belonging to the lowest energy docked model of the most populated cluster was selected as a reference structure for further analysis. The two predicted binding sites for malonyl-CoA were named as follows: the one close to the predicted site on the NH<sub>2</sub>-terminal domain and the acyl-CoA entrance was called the “A site” (for CoA site), and the other, on the opposite side of the molecule in the catalytic channel, was called the “O site” (for opposite-to-CoA site) (Fig. 2). Table 2 lists the residues predicted to be related to the malonyl-CoA binding to the enzyme.

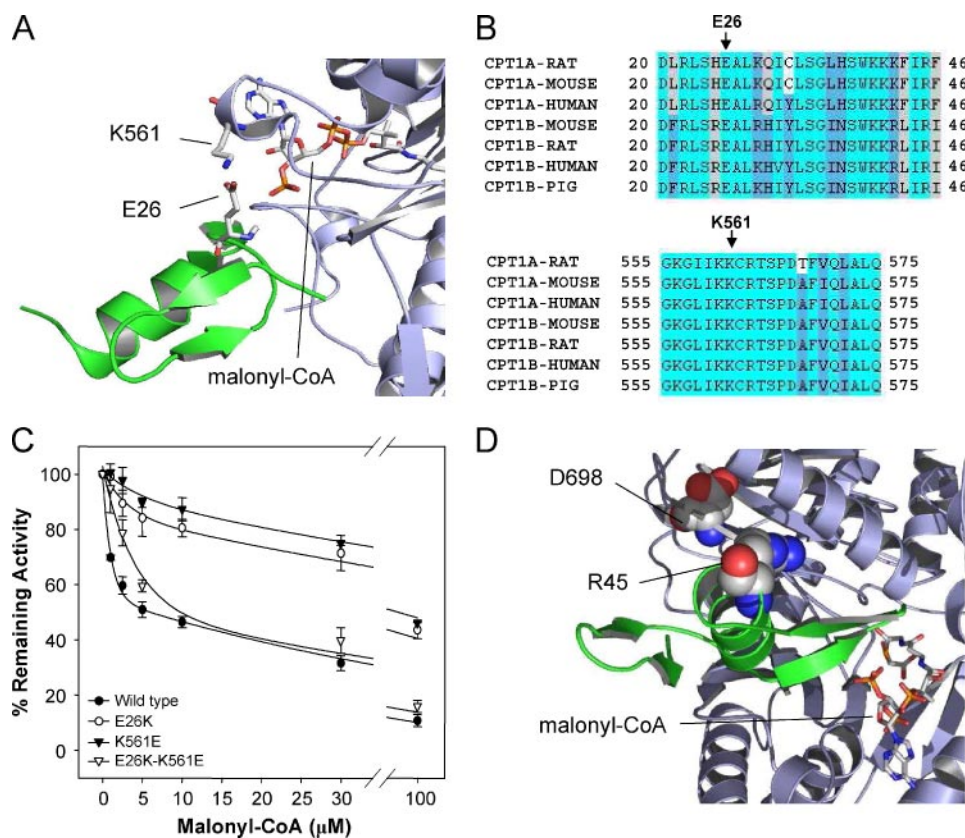
*Mutational Analysis of CPT1A NH<sub>2</sub>- and COOH-terminal Residues Predicted to be Involved in Malonyl-CoA Binding to the A Site*—To provide experimental support for the model of the interaction between NH<sub>2</sub>- and COOH-terminal domains and for the modeled location of malonyl-CoA contacting residues in both protein segments, some of the CPT1 residues at the interface were mutated, and their enzymatic activities were measured at different malonyl-CoA concentrations. A pair of interacting residues, Glu<sup>26</sup>-Lys<sup>561</sup>, was selected due to the clear electrostatic nature of their interaction (Table 1). Residue

TABLE 2

**Residues contacting inhibitor malonyl-CoA located in NH<sub>2</sub>- or COOH-terminal domains of human CPT1A**

Shown are amino acids located in the vicinity (less than 4 Å) of the putative A site and O site for malonyl-CoA classified according to their position in the NH<sub>2</sub>-terminal domain or in the A site and O site docking CoA grooves or the carnitine pocket of the C terminus of human CPT1A. Residues located in the enzyme catalytic site that contact both positions of malonyl-CoA in the proposed models are shown in boldface type.

Malonyl-CoA-contacting residues at human CPT1A A site			Malonyl-CoA-contacting residues at human CPT1A O site		
Carnitine pocket	A site docking CoA groove	N-terminal domain	Carnitine pocket	O site docking groove	
Tyr <sup>241</sup>	Lys <sup>556</sup>	Arg <sup>29</sup>	Tyr <sup>241</sup>	Ile <sup>240</sup>	Leu <sup>539</sup>
His <sup>473</sup>	Lys <sup>560</sup>	Ile <sup>31</sup>	His <sup>473</sup>	Arg <sup>243</sup>	Leu <sup>540</sup>
Asp <sup>477</sup>	Ser <sup>565</sup>		Asp <sup>477</sup>	Gly <sup>244</sup>	Ser <sup>685</sup>
Ala <sup>478</sup>	Asp <sup>567</sup>		Ala <sup>478</sup>	Arg <sup>245</sup>	Phe <sup>712</sup>
Tyr <sup>589</sup>	Glu <sup>590</sup>		Tyr <sup>589</sup>	Gly <sup>246</sup>	Gly <sup>713</sup>
Ala <sup>591</sup>	His <sup>640</sup>		Ala <sup>591</sup>	Leu <sup>248</sup>	Pro <sup>714</sup>
Ser <sup>592</sup>	Met <sup>643</sup>		Thr <sup>602</sup>	Asn <sup>251</sup>	Val <sup>715</sup>
Met <sup>593</sup>	Gln <sup>688</sup>		Arg <sup>655</sup>	Ser <sup>252</sup>	Lys <sup>739</sup>
Thr <sup>602</sup>	Pro <sup>690</sup>		Ser <sup>687</sup>		
Thr <sup>686</sup>	Gln <sup>691</sup>				
Ser <sup>687</sup>	Gln <sup>692</sup>				
Thr <sup>689</sup>					



**FIGURE 3. Specific contacts between COOH- and NH<sub>2</sub>-terminal domains are necessary for malonyl-CoA inhibition at the A site.** *A*, detail of the interaction between residues Glu<sup>26</sup> and Lys<sup>561</sup>, located at the NH<sub>2</sub>- and COOH-terminal domains of the protein, respectively. *B*, multiple sequence alignment of residues located in the vicinity of Glu<sup>26</sup> and Lys<sup>561</sup>, showing complete conservation of both residues in CPT1A and CPT1B sequences. *C*, effect of malonyl-CoA on the activity of CPT1A wild type (black circles), mutant E26K (open circles), mutant K561E (black triangles), and double mutant E26K/K561E (open triangles). CPT1A activity was measured, and data are expressed relative to control values in the absence of inhibitor (100%) as the mean of three independent experiments. *D*, detail of the residues Arg<sup>45</sup> and Asp<sup>698</sup> at the NH<sub>2</sub>- and COOH-terminal domains of the protein. The malonyl-CoA molecule is also shown.

Lys<sup>561</sup> of the COOH-terminal domain was seen to be in close proximity to Glu<sup>26</sup> of the NH<sub>2</sub>-terminal domain (Fig. 3A). Both residues are completely conserved across the NH<sub>2</sub>- and COOH-terminal structure-based sequence alignment (Fig. 3B). In the modeled three-dimensional structure of the COOH-terminal domain, Lys<sup>561</sup> is located in a loop between  $\alpha$  helices H14 and H15. In addition, Lys<sup>561</sup> would be fully exposed to solvent and does not appear to form salt bridges with any other COOH-terminal residue within the conserved catalytic core of CPT1A.

On the basis of the structural model, we predicted that mutation of Glu<sup>26</sup> to Lys and of Lys<sup>561</sup> to Glu would drastically alter the mutual recognition of interacting NH<sub>2</sub>- and COOH-terminal domain surfaces and strongly reduce malonyl-CoA sensitivity. To confirm these predictions, E26K and K561E single mutants and a double mutant (swap) E26K/K561E were generated and tested for CPT1A activity and malonyl-CoA inhibition. Results are shown in Fig. 3C. Single mutant E26K decreased malonyl-CoA sensitivity, producing an increase in the IC<sub>50</sub> from  $7.3 \pm 0.5 \mu\text{M}$  (wild type) to  $92.4 \pm 9 \mu\text{M}$ . Analogous results were observed for the CPT1A K561E mutant, whose IC<sub>50</sub> increased to  $88.1 \pm 6 \mu\text{M}$ . Double mutant E26K/K561E, which is the result of a swap, rescued the modified malonyl-CoA sensitivity of each single mutant (IC<sub>50</sub> was  $9.8 \pm 0.3$

$\mu\text{M}$ ). The specific activities of mutants E26K, K561E, and E26K/K561E were  $21.6 \pm 2.1$ ,  $22.8 \pm 2.5$ , and  $38.9 \pm 4.4$ , respectively, and were similar to CPT1A wild type ( $25.0 \pm 1.9 \text{ nmol}\cdot\text{min}^{-1}\cdot\text{mg}$  of protein<sup>-1</sup>). In addition, Western blot analysis showed that protein expression of single and double mutants was similar to the wild type (data not shown).

A second pair of residues, Arg<sup>45</sup> and Asp<sup>698</sup>, were subjected to double mutation on the basis of their complementary charge, although they were more than 15 Å apart in the proposed model of NH<sub>2</sub>- and COOH-terminal domain interaction (Fig. 3D). This mutation strategy was applied as a negative control to ensure that the relative position of the NH<sub>2</sub>- and COOH-terminal domains, as well as the contact surface between them, had been correctly defined in the model. Mutants R45D and D698R and the double mutant (swap) R45D/D698R were expressed in *S. cerevisiae*, and the mitochondrial extracts were assayed for CPT1 activity and malonyl-CoA inhibition. As expected, none of the three mutants displayed different activity or sensitivity from the wild type (data not shown), suggesting that neither amino acid participated in NH<sub>2</sub>- to COOH-terminal domain binding or malonyl-CoA location.

participated in NH<sub>2</sub>- to COOH-terminal domain binding or malonyl-CoA location.

*Mutation of Arg<sup>243</sup>, Located in the Second Predicted O Site for Malonyl-CoA, Diminished the Sensitivity of the Enzyme for the Inhibitor*—At the O site, up to 24 amino acid residues are within 4 Å of malonyl-CoA (Table 2). One of them, Arg<sup>243</sup>, was mutated to Thr<sup>243</sup>, the residue at the same position in CPT2, which is insensitive to malonyl-CoA. We reasoned that by altering the charge, we could prevent the positioning of malonyl-CoA. In the model, the positively charged Arg<sup>243</sup> lies close to the OH group in the pantothenic acid moiety of malonyl-CoA (Fig. 4A). Replacing it by the polar, albeit noncharged, threonine would be expected to modify the electrostatic characteristics of the surrounding area, thus preventing correct location of malonyl-CoA.

CPT1A mutant R243T was expressed in *S. cerevisiae* and tested for activity and malonyl-CoA inhibition. Results of the kinetic analysis are shown in Fig. 4. Apparent  $K_m$  values for carnitine and palmitoyl-CoA ( $56.3 \pm 2.9$  and  $7.0 \pm 2.2 \mu\text{M}$ ) of CPT1A R243T were similar to those of CPT1A wild type ( $59.7 \pm 2.5$  and  $3.6 \pm 0.4 \mu\text{M}$ ).  $V_{\text{max}}$  values for carnitine and palmitoyl-CoA were  $64.9 \pm 7.1$  and  $34.1 \pm 9.4 \mu\text{M}$  and  $70.6 \pm 10.3$  and  $36.3 \pm 6.9 \mu\text{M}$ , respectively, for CPT1A wild type and

## Two Separate Sites for Malonyl-CoA Inhibition of CPT1A

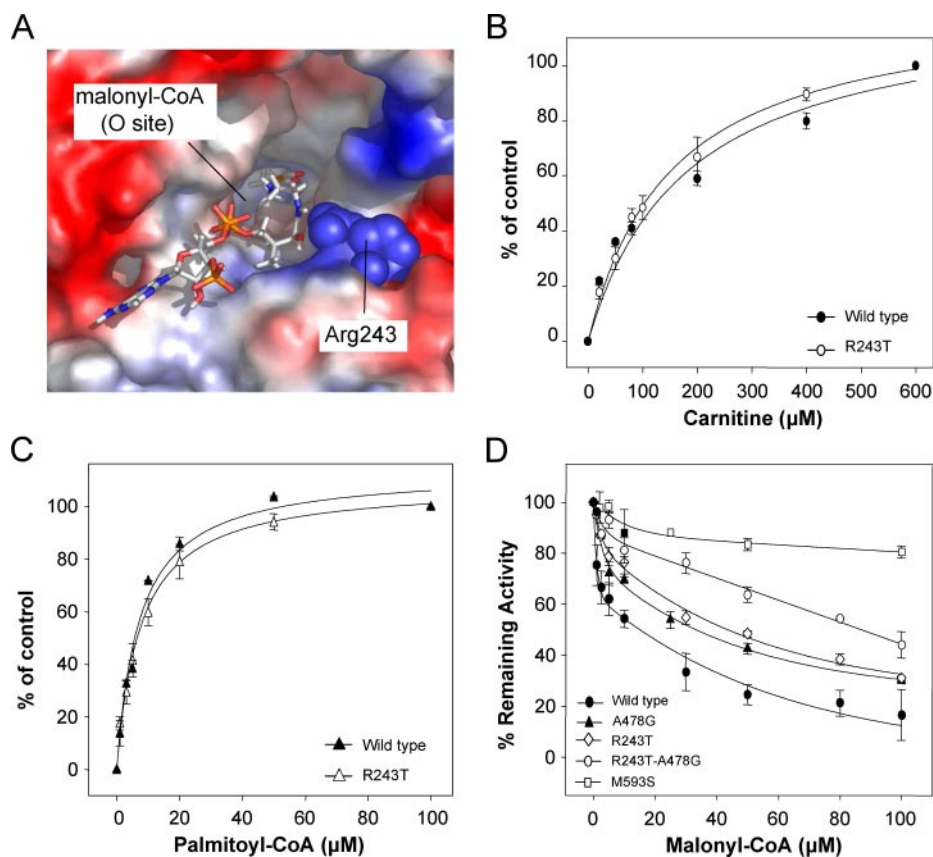


**FIGURE 4. CPT1A R243T mutant at the malonyl-CoA O site.** *A*, proposed location of malonyl-CoA molecule in the carnitine entrance O site of CPT1A surface. The position of residue Arg<sup>243</sup> is indicated, in close proximity with the inhibitor. *B* and *C*, kinetic analysis of the expressed wild type and mutant R243T of rat CPT1A. Isolated mitochondria from the yeast overexpressing wild type (●, ▲) and CPT1A R243T mutant (○, △) were assayed for CPT1 activity in the presence of increased carnitine and palmitoyl-CoA concentrations. The mean data from three to four curves obtained from separate yeast expressions are shown. *D*, effect of malonyl-CoA on the activity of yeast overexpressed wild type CPT1A (black circles), point mutants R243T (open rhombus), A478G (black triangles), and M593S (open squares) and double mutant R243T/A478G (open circles). Mitochondrially enriched fractions were incubated with increasing malonyl-CoA concentrations, and the enzyme activity was measured. Data are expressed relative to control values in the absence of inhibitor (100%) as the mean of three independent measurements. CPT1A M593S and CPT1A A478G mutants were previously reported (15).

mutant (Fig. 4, *B* and *C*). The  $IC_{50}$  malonyl-CoA value for CPT1A R243T was  $38.4 \pm 1.9 \mu\text{M}$ , showing lower malonyl-CoA sensitivity than the wild type ( $IC_{50} = 7.3 \pm 0.5 \mu\text{M}$ ).

According to Table 2, Ala<sup>478</sup> would be involved in both A site and O site for malonyl-CoA. Furthermore, previous studies had reported that the mutant CPT1A A478G showed reduced malonyl-CoA sensitivity ( $IC_{50} = 39.5 \pm 4.1 \mu\text{M}$ ) (15). To test whether a double mutation of residues Arg<sup>243</sup> and Ala<sup>478</sup> located far apart, one in the carnitine pocket and the other in the O site groove, could further decrease CPT1 malonyl-CoA sensitivity, we generated a double mutant. CPT1A R243T/A478G was expressed in *S. cerevisiae*, and the mitochondria-enriched fractions were tested for CPT1 activity and sensitivity to malonyl-CoA. CPT1A R243T/A478G showed a 20-fold increase in  $IC_{50}$  ( $IC_{50} > 150 \mu\text{M}$ ) with respect to the wild type protein ( $IC_{50} = 7.3 \pm 0.5 \mu\text{M}$ ), which is higher than those of the individual mutants but lower than that of the malonyl-CoA-insensitive CPT1A M593S ( $IC_{50} > 300 \mu\text{M}$ ) (15). Western blot analysis showed that protein expression levels from CPT1 mutants were similar to the wild type (data not shown).

*Malonyl-CoA and Carnitine Molecules Competed for the Same Location in the Active Center of CPT1A*—The positions of the residues in CPT1 predicted by the model (Fig. 2) indicate that carnitine and malonyl-CoA would compete for binding at both the A site and O site. To examine this hypothesis, we performed several studies based on results taken from the literature and on the measurement of inhibitory kinetics. We collected data on the  $IC_{50}$  for the inhibition of CPT1 by malonyl-CoA and the  $K_m$  for carnitine from publications by several laboratories. When we plotted  $\log IC_{50}$  (*y*) against  $\log K_m$  for carnitine (*x*), the result was a straight line. We classified the data from the literature as follows: 1) data from various tissues, such as rat liver, human fetal liver, rat heart, guinea pig liver, human skeletal muscle, rat skeletal muscle, dog skeletal muscle, and dog heart; 2) data from CPT1 cDNAs expressed in *Pichia pastoris* and data from CPT1 wild type and mutant cDNAs expressed in *S. cerevisiae* from our laboratory classified in two groups (one includes all mutants whose sensitivity to malonyl-CoA was virtually unchanged, and the other includes all mutants whose sensitivity to the inhibitor was nearly abolished). Logarithmic plots are represented in Fig. 5, *A* and *B*. In all cases, the linear equations have similar slopes, irrespective of the fact that 1) the CPT1 data were obtained from expression in two species of yeast, *P. pastoris* and *S. cerevisiae* (Fig. 5*B*); 2) the data were obtained from the cDNAs of the two isoforms CPT1A and CPT1B, (Fig. 5*B*); and 3) the data were obtained from diverse animal tissues (heart, skeletal muscle, and liver) and from various organisms (rat, human, and dog) (Fig. 5*A*). The average value for all slopes is as follows.

$$\frac{\Delta \log IC_{50} \text{ malonyl-CoA}}{\Delta \log K_m \text{ carnitine}} = -1.49 \pm 0.13 \quad (\text{Eq. 1})$$

We interpret this result as showing that malonyl-CoA and carnitine bind close to each other in the enzyme, and they repulse each other from the site of catalysis.

To further examine how carnitine interferes with malonyl-CoA inhibition, CPT1A wild type expressed in *S. cerevisiae* was assayed for activity and malonyl-CoA inhibition at carnitine concentrations of 100, 400, 800, and 1,600  $\mu\text{M}$  (Fig. 5*C*). The

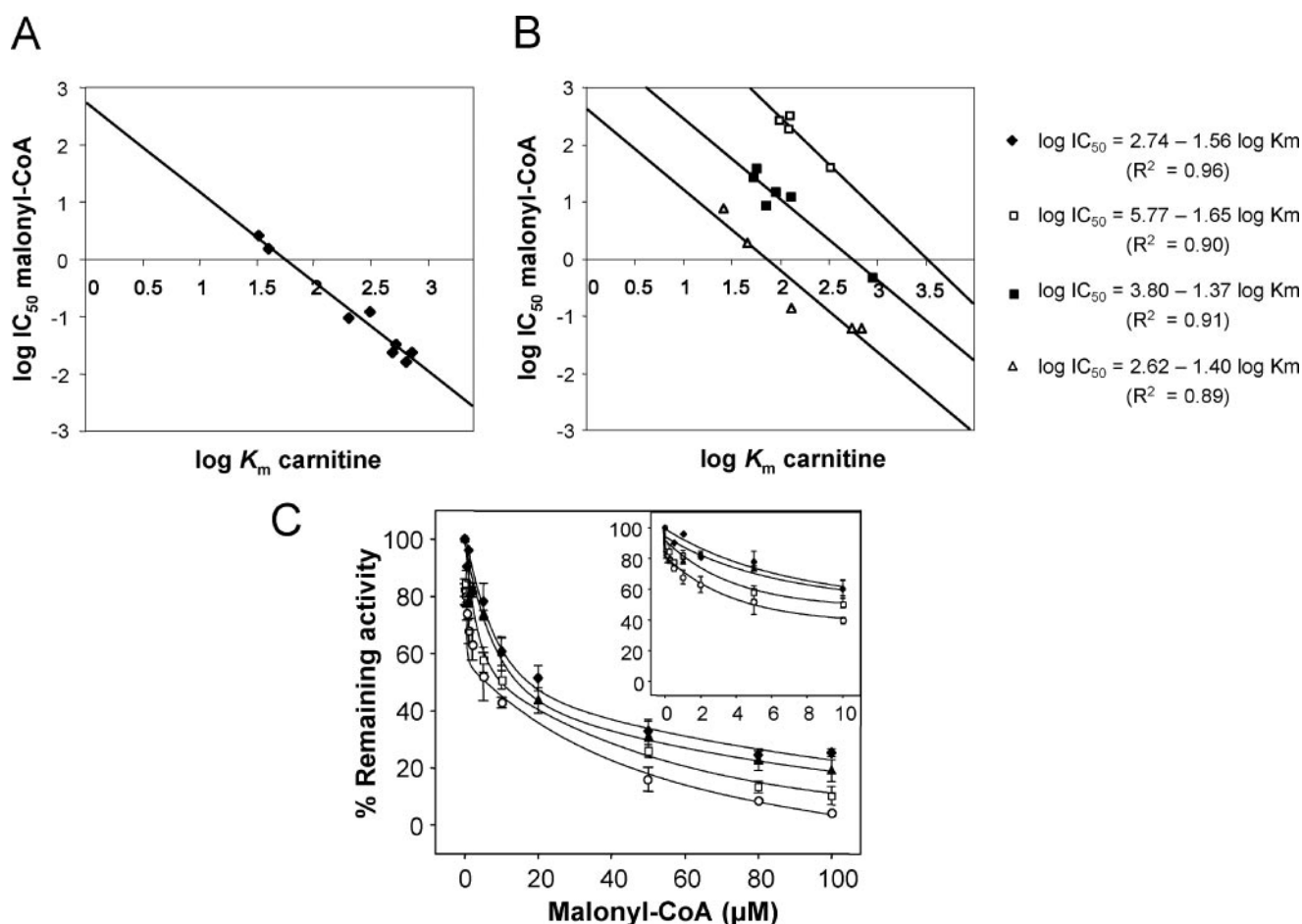


FIGURE 5. Kinetic analysis of wild type CPT1A inhibition by malonyl-CoA at different carnitine concentrations and linear relationship between  $\log IC_{50}$  from malonyl-CoA inhibition and  $\log K_m$  for carnitine. *A*, the data have been taken from literature (black diamonds) from rat liver, human fetal liver, rat heart, guinea pig liver, human skeletal muscle, rat skeletal muscle, dog skeletal muscle, and dog heart (22). *B*, the data are taken from rat and pig CPT1A wild type and human CPT1B wild type expressed in *P. pastoris* (open triangles) (12, 13, 54–56) and from rat CPT1 expressed in *S. cerevisiae*, either wild type and mutants (CPT1A wild type, CPT1B wild type, CPT1A T314S, CPT1A N464D, CPT1A C608A, and CPT1A R243T) that present unchanged sensitivity to malonyl-CoA (black squares) or CPT1 mutants (CPT1A H277A, CPT1A A478G, CPT1A M593S, and CPT1A T314S/N464D/A478G/M593S/C608A) that nearly abolish the sensitivity to the inhibitor (open squares) (15, 24). *C*, isolated mitochondria from yeast strain overexpressing wild type CPT1A were inhibited at increasing malonyl-CoA concentrations in the presence of various carnitine concentrations of 100  $\mu M$  (open circles), 400  $\mu M$  (open squares), 800  $\mu M$  (black triangles), and 1,600  $\mu M$  (black diamonds). Data are expressed relative to control values in the absence of inhibitor (100%) as the mean of three independent measurements. Inset, expanded dose-response curve for the inhibitor.

**TABLE 3**  
CPT1A activity and malonyl-CoA inhibition at increased carnitine concentrations

Yeast mitochondrial extracts overexpressing CPT1A were assayed for CPT1A activity and malonyl-CoA inhibition in the presence of 50  $\mu M$  palmitoyl-CoA and increasing concentrations of carnitine (as described under "Experimental Procedures"). CPT1A activity and  $IC_{50}$  values increased depending on increased carnitine concentrations.

Carnitine	CPT1A wild type activity	$IC_{50}$ malonyl-CoA
$\mu M$	$nmol \cdot min^{-1} \cdot mg^{-1}$	$\mu M$
100	$39.1 \pm 4.1$	$4.1 \pm 0.7$
400	$65.8 \pm 6.4$	$7.3 \pm 0.5$
800	$70.7 \pm 3.1$	$13.5 \pm 1.6$
1,600	$74.3 \pm 1.8$	$18.7 \pm 0.5$

curves show similar profiles, but inhibition was partially relieved at higher carnitine concentrations.  $IC_{50}$  values of inhibition by malonyl-CoA were progressively higher as carnitine concentration increased. The values were 4.3, 7.3, 13.5, and 18.7  $\mu M$  at carnitine concentrations of 100, 400, 800, and 1,600  $\mu M$ , respectively. These values correlate with the specific activity of the protein at each carnitine concentration (Table 3).

Another set of kinetic experiments was performed to identify the type of inhibition exerted by malonyl-CoA on CPT1A catalysis of carnitine. We performed experiments by varying malonyl-CoA and carnitine concentrations while maintaining palmitoyl-CoA and enzyme concentrations constant. The enzyme showed standard saturation kinetics for carnitine (Fig. 6A). Lineweaver-Burk plots for CPT1A activity were linear, and the  $K_m$  values observed for carnitine were 75.6, 80.9, and 102.9  $\mu M$  at malonyl-CoA concentrations of 0, 10, and 50  $\mu M$ , respectively (Table 4). Changes were observed in the intrinsic catalytic activity of the enzyme and in the catalytic efficiency (defined as  $V_{max}/K_m$  ratio). Increasing malonyl-CoA concentrations produced a decrease in  $V_{max}/K_m$  ratio (0.86, 0.49, and 0.22 for 0, 10, and 50  $\mu M$  malonyl-CoA, respectively), which indicates that CPT1A decreased its preference for carnitine when malonyl-CoA increased. This reduction is due to both the decrease in the  $V_{max}$  and the increase in the  $K_m$  value for carnitine, the former being the stronger factor. Lineweaver-Burk plots for CPT1A at differ-

## Two Separate Sites for Malonyl-CoA Inhibition of CPT1A

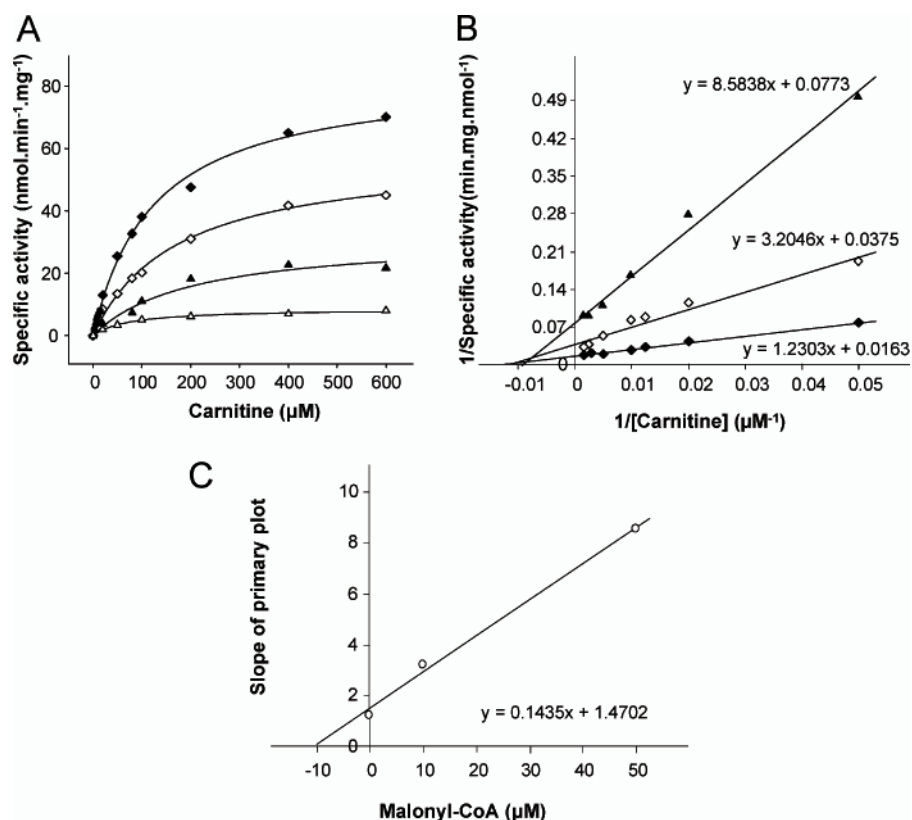
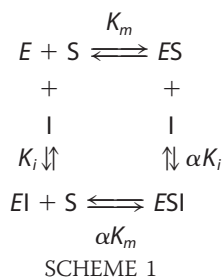


**FIGURE 6. Kinetic analysis of wild type CPT1A for carnitine as a substrate at different malonyl-CoA concentrations.** A, yeast extracts of 10 μg of protein were used for rat CPT1A activity. Shown is a Michaelis-Menten representation of activity versus increasing carnitine concentrations at four different malonyl-CoA levels: 0 μM (black diamonds), 10 μM (open diamonds), 50 μM (black triangles), and 100 μM (open triangles). B, Lineweaver-Burk plot of the kinetics shown in A. C, secondary plot of kinetic data from B. Data are the means of two separate experiments.

ent malonyl-CoA concentrations gave a set of straight lines intersecting to the *left* of the  $1/v$  axis but *above* the  $1/[\text{carnitine}]$  axis (Fig. 6B). Secondary plots of the slopes versus  $[I]$  and the  $1/v$  axis intercept versus  $[I]$  are linear (Fig. 6). Dixon plots of the inhibition data are also linear (data not shown). These kinetic results are compatible with linear mixed type inhibition and may be considered a mixture of partial competitive inhibition and pure noncompetitive inhibition, in which the ESI complex is catalytically inefficient. In this type of inhibition, there are two processes by which the inhibitor may bind to the enzyme and to the enzyme-substrate complex.



In this context, two inhibition constants appear:  $K_i$  and  $K_j = \alpha K_i$ . Hence,  $K_i = [E][I]/[EI]$  and  $\alpha K_i = [ES][I]/[ESI]$ .  $K_i$  is the dissociation constant of the enzyme-malonyl-CoA complex

and an indicator of the affinity of the enzyme for malonyl-CoA, and  $K_j$  refers to the enzyme-substrate-inhibitor complex. The Lineweaver-Burk equation for linear mixed inhibition can be written as follows.

$$\frac{1}{V} = \frac{1}{V_{\max(\text{app})}} + \frac{K_{m(\text{app})}}{V_{\max(\text{app})}} \times \frac{1}{[S]} \quad (\text{Eq. 2})$$

where

$$V_{\max(\text{app})} = \frac{V_{\max}}{\left(1 + \frac{I}{\alpha K_i}\right)} \quad (\text{Eq. 3})$$

and

$$K_{m(\text{app})} = K_m \times \frac{\left(1 + \frac{I}{K_i}\right)}{\left(1 + \frac{I}{\alpha K_i}\right)} \quad (\text{Eq. 4})$$

The value of  $\alpha K_i$  ( $K_j$ ) was obtained from the intercept on the  $[I]$  axis when we plotted  $1/V_{\max(\text{app})}$  against  $[I]$ . The value of  $K_i$  was obtained when we plotted the slopes of primary plots against  $[I]$  as the intercept on the  $[I]$  axis. The values obtained for  $K_j = \alpha K_i$  and  $K_i$  were  $13.2 \pm 1.4$  and  $10.6 \pm 0.8 \mu\text{M}$ , respectively, thus indicating that the value of  $\alpha$  is greater than 1 (in this case,  $\alpha = 1.24$ ), which is consistent with the intersection point position showed in Lineweaver-Burk plots.

However, our kinetic results are also compatible with inhibition produced by the binding of the inhibitor at two separate sites. Data from the present study and from other authors indicate that there are two malonyl-CoA binding sites. Therefore, the kinetic data should be discussed in terms of kinetic models based on two binding sites for malonyl-CoA. The first model would involve the following scheme that is a mixture of pure competitive and pure noncompetitive inhibition (Scheme 2).

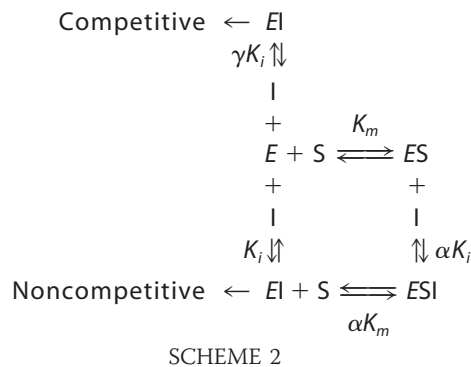


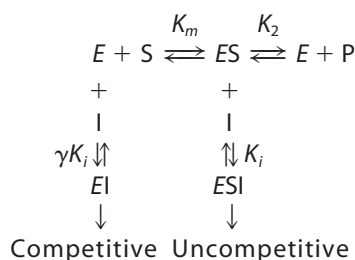
TABLE 4

Kinetic parameters of CPT1A expressed in *S. cerevisiae*

Mitochondrial enriched fractions from yeast overexpressed CPT1A were assayed at different malonyl-CoA concentrations with palmitoyl-CoA and carnitine, as described under "Experimental Procedures." Results are the mean  $\pm$  S.D. of at least three independent experiments. ND, not determined.

Malonyl-CoA	CPT1A wild type activity	Carnitine		Catalytic efficiency ( $V_{\max}/K_m$ )
		Observed $K_m$	Observed $V_{\max}$	
$\mu\text{M}$	$\text{nmol}\cdot\text{min}^{-1}\cdot\text{mg}^{-1}$	$\mu\text{M}$	$\text{nmol}\cdot\text{min}^{-1}\cdot\text{mg}^{-1}$	
0	$65.8 \pm 6.4$	$75.6 \pm 0.6$	$65.4 \pm 4.4$	0.86
10	$42.2 \pm 14.3$	$80.9 \pm 4.4$	$40.1 \pm 13.5$	0.49
50	$22.9 \pm 11.5$	$102.9 \pm 8.0$	$22.9 \pm 10.0$	0.22
100	$7.3 \pm 0.2$	ND	ND	ND

Calculations from the data obtained gave the following results:  $\alpha K_i = 13.2$  and  $\gamma K_i/1 + \gamma = 10.6$ . If  $\alpha = 1$ , therefore,  $K_i = 13.2$  and  $\gamma = 4.1$ . The second model would correspond to the following scheme (*i.e.* a mixture of pure competitive and pure uncompetitive inhibition) (Scheme 3).



SCHEME 3

Calculations from the data obtained gave the following results:  $\gamma = 0.80$ , when  $K_i = 13.2$ .

At this point, we cannot predict which of the two models would better fit CPT1A; both models support the kinetic data obtained for  $V_{\max}$  and  $K_m$  at the malonyl-CoA and carnitine concentrations assayed.

## DISCUSSION

Despite several efforts to characterize CPT1, its mode of action is not yet completely understood, probably due to the difficulty of obtaining an appropriate crystal, since it is an integral membrane protein. The aim of this study was to develop a structural model of the  $\text{NH}_2$ -terminal domain and to examine its interactions with the C-terminal domain in order to predict the location of malonyl-CoA in CPT1 enzyme and its ability to interact with the substrates carnitine and palmitoyl-CoA. We present, for the first time, a partial bioinformatic model of the  $\text{NH}_2$ -terminal domain, which lacks only the first 9 amino acids. Unfortunately, the very first residues in the  $\text{NH}_2$ -terminal domain cannot be modeled due to the lack of a feasible template. Thus, we cannot explain the role of several residues located in this segment, like Glu<sup>3</sup> or His<sup>5</sup>, previously implicated in sensitivity to malonyl-CoA. Nevertheless, the spatial position of the first modeled residues at the  $\text{NH}_2$ -terminal end suggests that the first 9 residues could be allocated close to, or in contact with, the surface of the COOH-terminal modeled structure. In an earlier attempt to predict part of the  $\text{NH}_2$ -terminal domain structure, it was proposed that the residues within region 19–31 had an  $\alpha$ -helical structure (16). However, this predicted  $\alpha$ -helical structure does not match the  $\alpha$ -helix (residues 38–48) of our  $\text{NH}_2$ -terminal model. Whereas the predicted

$\alpha$ -helical structure was based only on amino acid sequence, our model is based on both amino acid sequence and structural homology. Our  $\text{NH}_2$ -terminal model includes not only an  $\alpha$ -helix but also four  $\beta$ -strands. The segment comprising  $\beta$  strands 3 and 4 has a lower confidence index than the surrounding amino acids, since in this region the modeling procedures have rebuilt a missing inner loop region not present in the structural template 1TF3. Although we cannot affirm that this conformation and its secondary structure assignment reflect the true domain structure, the model seems self-consistent according to the continuity of the  $\alpha$ -carbon backbone trace and the favorable interactions within the force field energy of the  $\text{NH}_2$ -terminal model.

Interestingly, the topology of the *in silico* modeled  $\text{NH}_2$ -terminal domain of CPT1A resembles the characteristic subdomain (residues 175–210, containing two flanking  $\beta$ -strands plus two  $\alpha$ -helices) present in the CPT2 structure (33, 47), which mimics the interactions of the  $\text{NH}_2$ -domain with the COOH-terminal domain. Furthermore, the *in silico* docking model of  $\text{NH}_2$ - and COOH-terminal domains suggests specific interactions between them. The main set of contacting residues can be mapped onto the surface of the CPT1A COOH-terminal domain and, to a lesser extent, the  $\text{NH}_2$ -terminal domain. A pair of residues, (Glu<sup>26</sup>-Lys<sup>561</sup>), located in the  $\text{NH}_2$ - and COOH-terminal domain, respectively, were selected for mutation, because their side chains could form a saline bridge between their functional groups. The decrease in the malonyl-CoA sensitivity of these point mutants could be a result of the disturbed electrostatic interactions between their charged side chains. Moreover, the recovery of malonyl-CoA sensitivity of the double mutant (swap) suggests that the relative position of  $\text{NH}_2$ - and COOH-terminal domains bound to each other is more important in terms of overall functionality than the individual nature of the residues involved in the interaction, an evolutionary phenomenon known as correlated mutations (48). In contrast to the loss of sensitivity to malonyl-CoA, point mutants did not show any change in CPT1 activity, which suggests that this contact between  $\text{NH}_2$ - and COOH-terminal domains is not important for activity. This is consistent with previous studies, in which deletions between residues 19 and 30 did not change CPT1A activity (17). Other important interactions are highlighted by the model. It predicts the positioning of Leu<sup>28</sup> ( $\text{NH}_2$ -terminal domain) mostly sheathed by the hexanoyl fragments of Lys<sup>556</sup> and Lys<sup>560</sup> side chains (COOH-terminal domain). Leu<sup>28</sup> is fully conserved in CPT1A and CPT1B members, and it could be involved in positioning the positive net charge of the two lysine residues on the binding surface of the

## Two Separate Sites for Malonyl-CoA Inhibition of CPT1A

COOH-terminal domain. Leu<sup>28</sup> is in close proximity to the ribose in the CoA moiety of palmitoyl-CoA. Regarding the nucleotide moiety of the palmitoyl-CoA, residues Lys<sup>556</sup> and Lys<sup>560</sup> would be fully exposed to the solvent and in contact with the phosphate group attached to the nucleoside ribose in the CoA moiety. Both lysine residues flank  $\alpha$  helix H14 and are fully conserved in all members of the carnitine acyltransferase family, which suggests a conserved electrostatic-mediated interaction between charged lysine residues and phosphate functional groups in CoA-based ligands. The mutant K560A showed less activity than the wild type (49), probably due to a decrease in the CPT 1 binding stability of the CoA substrates.

The model also predicts a contact between malonyl-CoA and the NH<sub>2</sub>-terminal domain via Arg<sup>29</sup>, which could establish a polar interaction with the hydroxyl group of the ribose in the CoA fragment of the inhibitor. The alkaline character of this amino acid is conserved in CPT1A and CPT1B. The palmitoyl-CoA substrate and the inhibitor would occupy the same position in the "A site." Several authors (7–13) have reported that malonyl-CoA binds to CPT1 at two separate sites, with low and high affinity. The low affinity binding site is the locus at which palmitoyl-CoA and malonyl-CoA compete (50). The A site proposed in the present study would be compatible with this low affinity site. Natural endobiotics like free CoA, acetyl-CoA, and propionyl-CoA inhibit CPT1 by binding at the acyl-CoA (51). The A site would correspond to those molecules that need coenzyme A to bind. CoA would position their acidic moieties at their final location. This site would be distinct from the other malonyl-CoA binding site described by enzymatic methods.

On the basis of our *in silico* docking experiments, an additional locus, the "O site," for malonyl-CoA positioning was proposed, which is located on the opposite side of the molecule. This site might correspond to the proposed second malonyl-CoA binding site exclusive to the inhibitor (50). In this locus, the interaction of malonyl-CoA with the enzyme would mostly depend on the dicarbonyl group (CO-CH<sub>2</sub>-CO or CO-CO structures) rather than on interactions of the CoA itself with its surrounding amino acids. Kashfi and Cook (51) have shown that molecules with a dicarbonylic structure (among them, 4-hydroxyphenylglyoxylate and Ro 25-0187) inhibit CPT1 activity to varying degrees by binding to a specific malonyl-CoA binding site, which is quite different from the acyl-CoA binding site. When we performed *in silico* docking studies of Ro 25-0187 on our CPT1A model, we observed a significant preference, in terms of energy stabilization, for the O site over the A site (data not shown). Other compounds with both a dicarbonylic structure and a CoA moiety, such as succinyl-CoA and methylmalonyl-CoA (52) interact with a second specific malonyl-CoA-inhibitory binding site. The coenzyme A moiety of these molecules may increase the potency of these weak inhibitors. However, high potency inhibitors like Ro 25-0187 did not need to be in the form of coenzyme A ester, suggesting that the dicarbonylic structure is responsible for their inhibitory effect.

The docking model also shows that the side chain of residue Arg<sup>243</sup> is exposed to the solvent in the O site, far from the central catalytic hollow occupied by carnitine. Arg<sup>243</sup> is completely conserved in all CPT1 members. This residue would establish polar contacts with the CoA moiety of malonyl-CoA,

putatively through the hydroxyl group of the pantothenic fragment of the inhibitor. Mutation of Arg<sup>243</sup> to Thr did not affect CPT1 activity but slightly diminished enzyme sensitivity to malonyl-CoA, thus supporting this O site position. The double mutant CPT1A R243T/A478G was less sensitive to malonyl-CoA than the single mutants. This is caused by the sum of the specific interactions of each residue with the inhibitor, since they are far from each other in the tunnel. The differential surrounding amino acidic composition of the A site and O site indicates that malonyl-CoA could establish a different network of polar and nonpolar interactions with differential stability upon binding. However, a single hydrophobic residue Met<sup>593</sup>, conserved in all carnitine-acyltransferases susceptible to inhibition by malonyl-CoA, is essential to malonyl-CoA sensitivity (15), although the mechanistic details of its role in the enzyme active center remains still elusive.

From the kinetic data presented (Fig. 6), we conclude that only one of the two inhibition sites is competitive with respect to the substrate carnitine and that the two inhibitory sites are mutually exclusive, showing different affinity for malonyl-CoA. There are two possible explanations for the kinetic data (Schemes 2 and 3); in both cases, the binding of malonyl-CoA to one inhibitory site excludes the binding of carnitine. In Scheme 2, the binding of malonyl-CoA at the second site is independent of the binding of carnitine, whereas in Scheme 3, this binding would be possible only if carnitine was already bound (53). We are not yet in a position to decide which model is the more accurate.

In the present article, we have taken the data from various authors who studied the relationships between IC<sub>50</sub> for malonyl-CoA and  $K_m$  of carnitine under different conditions and attempted to find a formula that might link them. It is noteworthy that, despite the wide variety of sources of data, the relationship between log IC<sub>50</sub> for malonyl-CoA inhibition and log  $K_m$  for carnitine is linear, and the slope is essentially the same (values range between -1.37 and -1.65, with a mean value of -1.49). Kinetic data indicate that malonyl-CoA interferes with the carnitine binding and thus that their respective binding sites are close. Moreover, kinetic experiments performed in this study confirm this hypothesis. It was observed that in yeast-expressed wild type CPT1A, an increase in carnitine concentration produced an increase in IC<sub>50</sub> values for malonyl-CoA (Fig. 5C and Table 3). Equally, when kinetics experiments were performed by varying carnitine concentrations at several fixed malonyl-CoA levels, Michaelis-Menten hyperbolic kinetics were obtained in which the apparent  $K_m$  for carnitine increased at progressively higher malonyl-CoA concentrations.

Kinetic results also agree with the *in silico* model for two possible binding sites for malonyl-CoA that would be situated along the catalytic tunnel, from the carnitine hollow where the catalytic His<sup>473</sup> lies, toward the opposite distal surfaces of CPT1. The docked malonyl-CoA model in the A site shows polar contacts at the carnitine-binding site with the conserved residues Tyr<sup>241</sup>, His<sup>473</sup>, Asp<sup>477</sup>, Ala<sup>478</sup>, Tyr<sup>589</sup>, Thr<sup>602</sup>, Ser<sup>685</sup>, and Ser<sup>687</sup> (as shown in Table 2). The catalytic His<sup>473</sup> (24) would make contact with the carboxyl group of malonyl-CoA, suggesting a possible electrostatic interaction between them. Other polar contacts between malonyl-CoA carboxylic oxygen

atoms and CPT1A include Tyr<sup>241</sup>, Tyr<sup>589</sup>, and Thr<sup>602</sup> hydroxyl groups. Most, but not all, of the residues in the carnitine hollow are shared by the A site and the O site (Table 2).

From the data presented in this study, can we deduce the stoichiometry between malonyl-CoA and CPT1? Data from Fig. 2 indicate that the two malonyl-CoA molecules compete for the same space within the catalytic site. This would support a functional (malonyl-CoA/CPT1A) 1:1 stoichiometry. On the other hand, a 2:1 stoichiometry in our kinetic study would entail that a putative  $EI_2$  complex would give a pattern of straight lines that would not intersect at the same point in a double reciprocal values plot (this is not the case) and also that the secondary representation (slopes *versus* [I]) would produce a parabola. These graphics have not been obtained in our study, from which a 1:1 stoichiometry of malonyl-CoA/CPT1A was suggested.

To our knowledge, no quantitative stoichiometry has been presented elsewhere in the literature. Several biochemical studies, however, have shown that malonyl-CoA binds in two sites: one high affinity and the other low affinity. Scatchard plots of [<sup>14</sup>C]malonyl-CoA binding in the liver CPT1 isoform clearly show that there are two, kinetically distinguishable malonyl-CoA binding sites (10, 50, 57). However, in 1990, Kolodziej and Zammit (58) re-evaluated the interaction of malonyl-CoA with the rat liver mitochondrial CPT1 system by using purified outer membranes. From the Scatchard plots, they concluded that malonyl-CoA binding was largely accounted for by a single, high affinity component in CPT1, in contrast to the dual site previously found with intact mitochondria. They suggested that the low affinity binding observed with intact rat liver mitochondria may be totally unrelated to the CPT1 system and may be associated with other proteins present in the mitochondrial intermembrane space or inner membrane as well as other structures that contaminate crude mitochondrial preparations (peroxisomes and microsomes). This would suggest a malonyl-CoA/CPT1A stoichiometry of 1:1. Moreover, Cook *et al.* (7), through a Yonetani-Theorell analysis of liver CPT1 inhibition with two CPT1 inhibitors (malonyl-CoA and free CoA), showed that every one binds to a different site, from which it could be inferred that the stoichiometry of CPT1/malonyl-CoA/free CoA could be 1:1:1. This view would support our three-dimensional model, since free CoA could freely bind on the A site without steric hindrance to the simultaneous malonyl-CoA binding in the O site. Our three-dimensional model, in addition, allows the binding of a malonyl-CoA on the O site simultaneous with the palmitoyl-CoA binding on the A site. This view would also be supported by the data by Kolodziej and Zammit (58), which showed that the occurrence of palmitoyl-CoA in the assay had no effect on the maximal binding capacity of [<sup>14</sup>C]malonyl-CoA on rat liver mitochondria. In this case, the stoichiometry would be as follows: 1:1:1 (CPT1A/malonyl-CoA/palmitoyl-CoA).

In a different study, Zammit and Corstorphine (57) also suggested that the microenvironment of the molecular species responsible for low affinity binding of malonyl-CoA undergoes temperature-related transitions that may derive from changes in membrane fluidity that occur around 25 °C, and evidently only binding at the high affinity site was required to elicit inhi-

bition of CPT1. In other words, temperature might modify the membrane fluidity, and as a consequence, the tertiary structure of CPT could be modified in such a way as to accept, under special circumstances, the second malonyl-CoA molecule in the (second) low affinity site.

In conclusion, we have located malonyl-CoA binding sites by *in silico* procedures, and they have been confirmed by site-directed mutagenesis of those amino acid residues interacting with the inhibitor. Moreover, individual mutations of critical amino acids (Glu<sup>26</sup> and Lys<sup>561</sup>) reduced malonyl-CoA sensitivity, showing the precise interactions between NH<sub>2</sub>- and COOH-terminal domains. However, when the interaction was preserved in a double mutant, in which the individual positions were swapped (whether NH<sub>2</sub>- or COOH-terminal), malonyl-CoA sensitivity was rescued. This study also shows that the relationship between malonyl-CoA and carnitine is mutually exclusive, as deduced from the docking position of both carnitine and malonyl-CoA in the three-dimensional model of CPT1. The inhibitory kinetic studies are also compatible with this view.

*Acknowledgments*—We are grateful to Robin Rycroft of the Language Service for valuable assistance in the preparation of the manuscript and to Biomol-Informatics SL for bioinformatics consulting.

## REFERENCES

- McGarry, J. D., and Brown, N. F. (1997) *Eur. J. Biochem.* **244**, 1–14
- Esser, V., Britton, C. H., Weis, B. C., Foster, D. W., and McGarry, J. D. (1993) *J. Biol. Chem.* **268**, 5817–5822
- Yamazaki, N., Shinohara, Y., Shima, A., and Terada, H. (1995) *FEBS Lett.* **363**, 41–45
- Price, N., van der Leij, F., Jackson, V., Corstorphine, C., Thomson, R., Sorensen, A., and Zammit, V. (2002) *Genomics* **80**, 433–442
- Anderson, R. C. (1998) *Curr. Pharm. Des.* **4**, 1–16
- Cha, S. H., Rodgers, J. T., Puigserver, P., Chohan, S., and Lane, M. D. (2006) *Proc. Natl. Acad. Sci. U. S. A.* **103**, 15410–15415
- Cook, G. A., Mynatt, R. L., and Kashfi, K. (1994) *J. Biol. Chem.* **269**, 8803–8807
- Zammit, V. A., Corstorphine, C. G., and Gray, S. R. (1984) *Biochem. J.* **222**, 335–342
- Zammit, V. A. (1984) *Biochem. J.* **218**, 379–386
- Bird, M. I., and Saggerson, E. D. (1984) *Biochem. J.* **222**, 639–647
- Bird, M. I., and Saggerson, E. D. (1985) *Biochem. J.* **230**, 161–167
- Shi, J., Zhu, H., Arvidson, D. N., and Woldegiorgis, G. (1999) *J. Biol. Chem.* **274**, 9421–9426
- Shi, J., Zhu, H., Arvidson, D. N., and Woldegiorgis, G. (2000) *Biochemistry* **39**, 712–717
- Jackson, V. N., Cameron, J. M., Fraser, F., Zammit, V. A., and Price, N. T. (2000) *J. Biol. Chem.* **275**, 19560–19566
- Morillas, M., Gomez-Puertas, P., Benteibibel, A., Selles, E., Casals, N., Valencia, A., Hegardt, F. G., Asins, G., and Serra, D. (2003) *J. Biol. Chem.* **278**, 9058–9063
- Jackson, V. N., Price, N. T., and Zammit, V. A. (2001) *Biochemistry* **40**, 14629–14634
- Jackson, V. N., Zammit, V. A., and Price, N. T. (2000) *J. Biol. Chem.* **275**, 38410–38416
- Faye, A., Borthwick, K., Esnous, C., Price, N. T., Gobin, S., Jackson, V. N., Zammit, V. A., Girard, J., and Prip-Buus, C. (2005) *Biochem. J.* **387**, 67–76
- Borthwick, K., Jackson, V. N., Price, N. T., and Zammit, V. A. (2006) *J. Biol. Chem.* **281**, 32946–32952
- McGarry, J. D., Robles-Valdes, C., and Foster, D. W. (1975) *Proc. Natl. Acad. Sci. U. S. A.* **72**, 4385–4388
- Saggerson, E. D., and Carpenter, C. A. (1981) *FEBS Lett.* **129**, 225–228

## Two Separate Sites for Malonyl-CoA Inhibition of CPT1A

22. McGarry, J. D., Mills, S. E., Long, C. S., and Foster, D. W. (1983) *Biochem. J.* **214**, 21–28
23. Mills, S. E., Foster, D. W., and McGarry, J. D. (1984) *Biochem. J.* **219**, 601–608
24. Morillas, M., Gomez-Puertas, P., Roca, R., Serra, D., Asins, G., Valencia, A., and Hegardt, F. G. (2001) *J. Biol. Chem.* **276**, 45001–45008
25. Jaroszewski, L., Rychlewski, L., and Godzik, A. (2000) *Protein Sci.* **9**, 1487–1496
26. Jaroszewski, L., Rychlewski, L., Li, Z., Li, W., and Godzik, A. (2005) *Nucleic Acids Res.* **33**, W284–W288
27. Altschul, S. F., Madden, T. L., Schaffer, A. A., Zhang, J., Zhang, Z., Miller, W., and Lipman, D. J. (1997) *Nucleic Acids Res.* **25**, 3389–3402
28. Andreeva, A., Howorth, D., Brenner, S. E., Hubbard, T. J., Chothia, C., and Murzin, A. G. (2004) *Nucleic Acids Res.* **32**, D226–D229
29. Murzin, A. G., Brenner, S. E., Hubbard, T., and Chothia, C. (1995) *J. Mol. Biol.* **247**, 536–540
30. Berman, H. M., Westbrook, J., Feng, Z., Gilliland, G., Bhat, T. N., Weissig, H., Shindyalov, I. N., and Bourne, P. E. (2000) *Nucleic Acids Res.* **28**, 235–242
31. Foster, M. P., Wuttke, D. S., Radhakrishnan, I., Case, D. A., Gottesfeld, J. M., and Wright, P. E. (1997) *Nat. Struct. Biol.* **4**, 605–608
32. Jogl, G., Hsiao, Y. S., and Tong, L. (2005) *J. Biol. Chem.* **280**, 738–744
33. Hsiao, Y. S., Jogl, G., Esser, V., and Tong, L. (2006) *Biochem. Biophys. Res. Commun.* **346**, 974–980
34. Guex, N., Diemand, A., and Peitsch, M. C. (1999) *Trends Biochem. Sci.* **24**, 364–367
35. Peitsch, M. C. (1996) *Biochem. Soc. Trans.* **24**, 274–279
36. Schwede, T., Kopp, J., Guex, N., and Peitsch, M. C. (2003) *Nucleic Acids Res.* **31**, 3381–3385
37. Hooft, R. W., Vriend, G., Sander, C., and Abola, E. E. (1996) *Nature* **381**, 272
38. Vriend, G. (1990) *J. Mol. Graph.* **8**, 52–56
39. Guex, N., and Peitsch, M. C. (1997) *Electrophoresis* **18**, 2714–2723
40. Ritchie, D. W., and Kemp, G. J. (2000) *Proteins* **39**, 178–194
41. Goodsell, D. S., and Olson, A. J. (1990) *Proteins* **8**, 195–202
42. Morris, G. M., Goodsell, D. S., Halliday, R. S., Huey, R., Hart, E., Belew, R. K., and Olson, A. J. (1998) *J. Comput. Chem.* **19**, 1639–1662
43. Morris, G. M., Goodsell, D. S., Huey, R., and Olson, A. J. (1996) *J. Comput. Aided Mol. Des.* **10**, 293–304
44. Cordente, A. G., Lopez-Vinas, E., Vazquez, M. I., Swiegers, J. H., Pretorius, I. S., Gomez-Puertas, P., Hegardt, F. G., Asins, G., and Serra, D. (2004) *J. Biol. Chem.* **279**, 33899–33908
45. Benteibibel, A., Sebastian, D., Herrero, L., Lopez-Vinas, E., Serra, D., Asins, G., Gomez-Puertas, P., and Hegardt, F. G. (2006) *Biochemistry* **45**, 4339–4350
46. Stewart, J. J. (1990) *J. Comput. Aided Mol. Des.* **4**, 1–105
47. Rufer, A. C., Thoma, R., Benz, J., Stihle, M., Gsell, B., De Roo, E., Banner, D. W., Mueller, F., Chomienne, O., and Hennig, M. (2006) *Structure* **14**, 713–723
48. Tress, M., de Juan, D., Grana, O., Gomez, M. J., Gomez-Puertas, P., Gonzalez, J. M., Lopez, G., and Valencia, A. (2005) *Proteins* **60**, 275–280
49. Morillas, M., Lopez, V. E., Valencia, A., Serra, D., Gomez-Puertas, P., Hegardt, F. G., and Asins, G. (2004) *Biochem. J.* **379**, 777–784
50. Grantham, B. D., and Zammit, V. A. (1986) *Biochem. J.* **233**, 589–593
51. Kashfi, K., and Cook, G. A. (1999) *Adv. Exp. Med. Biol.* **466**, 27–42
52. Kashfi, K., Mynatt, R. L., and Cook, G. A. (1994) *Biochim. Biophys. Acta* **1212**, 245–252
53. Segel, I. H. (1993) *Enzyme Kinetics: Behavior and Analysis of Rapid Equilibrium and Steady State Enzyme Systems*, pp. 170–192, John Wiley & Sons, Inc., New York
54. Esser, V., Brown, N. F., Cowan, A. T., Foster, D. W., and McGarry, J. D. (1996) *J. Biol. Chem.* **271**, 6972–6977
55. Nicot, C., Hegardt, F. G., Woldegiorgis, G., Haro, D., and Marrero, P. F. (2001) *Biochemistry* **40**, 2260–2266
56. Zhu, H., Shi, J., de Vries, Y., Arvidson, D. N., Cregg, J. M., and Woldegiorgis, G. (1997) *Arch. Biochem. Biophys.* **347**, 53–61
57. Zammit, V. A., and Corstorphine, C. G. (1985) *Biochem. J.* **231**, 343–347
58. Kolodziej, M. P., and Zammit, V. A. (1990) *Biochem. J.* **267**, 85–90